Tribology International 190 (2023) 109060

Contents lists available at ScienceDirect

Tribology International

journal homepage: www.elsevier.com/locate/triboint

Enhancing physicochemical properties of coconut oil for the application of engine lubrication

Sunil Jayantha Hettiarachchi [a], Suela Kellici [a], Matthew Kershaw [b], James Bowen [b,*]

[a] London Centre for Energy Engineering, School of Engineering, London South Bank University, London SE1 0AA, UK
[b] Faculty of Science, Technology, Engineering, and Mathematics, Open University, Milton Keynes MK7 6AA, UK

ARTICLE INFO

Keywords:
Coconut oil
Oxidative stability
Pour point depressants
Shear stability
Thermal stability
Total base number
Viscosity modifiers

ABSTRACT

Engine lubricants require specific physical and chemical properties to function effectively and extend the lifespan of engines. Coconut oil (CCO) is an abundant, renewable, and environmentally friendly bio-based stock that has the potential to be a viable alternative to conventional mineral oil-based lubricants. In this study, we investigated the potential of CCO as a lubricant and formulated different blends with additives to enhance its physicochemical characteristics. Polymethylmethacrylate (PMMA), styrenated phenol (SP) and potassium hydroxide (KOH) were used as additives in varying concentrations. We evaluated the formulations for low pour point (PP), high viscosity index (VI) and total base number (TBN) using differential scanning calorimetry (DSC), viscometry, and titration methods (following ASTM D2270 and ASTM D2896–21 respectively). The formulated CCO was also tested for thermal, oxidative, and shear stability using thermogravimetric analysis and rheometry. The optimal formulation exhibited a PP reduction from 21 °C to 6 °C, improved VI from 169 to 206, and a TBN adjustment from 0 to 4.14 mg KOH g^{-1}. The formulated CCO also exhibited superior thermal, oxidative, and shear stability compared to unformulated CCO and reference oil (15W40). Our results suggest that blending CCO with additives can effectively enhance its suitability for engine lubrication, opening up new possibilities for environmentally sustainable and renewable lubricants.

1. Introduction

The contemporary lubricant industry is increasingly receptive toward the production of bio-based lubricants to mitigate growing environmental concerns. Bio-lubricants have been proven to have superior biodegradability, lower toxicity, higher viscosity index, and to be more recyclable and renewable compared to mineral-based lubricants, and are thus good candidates to substitute mineral-based lubricants [1]. Nonetheless, one of the limitations observed for bio-lubricants is low-temperature characteristics; wax formation, poor cold flow, high pour point (PP), and low oxidative stability are the qualities in need of enhancement [1,2], which this work aims to resolve. Numerous bio-lubricants containing plant oils or animal fats are in use with reasonably similar molecular structures belonging to the class commonly known as triglycerides [1]. Coconut oil (CCO) is an eco-friendly edible plant oil with excellent availability; global CCO production is 3.5×10^9 kg/year [3], and hence CCO has been selected in this work as the bio-based stock. Thus, the aims of this research are to a) reduce the PP, b) improve oxidative stability, and c) consider other related physicochemical properties of CCO for the application of engine lubrication.

CCO has a kinematic viscosity of 5.5 $mm^2 s^{-1}$ at 100 °C, total acid number (TAN) of 1.99 ~ 12.8 mg KOH g^{-1}, and pour point (PP) of 21 ~ 24 °C: below this temperature, the oil is solid and unable to flow [1,2,4,5]. These characteristics are the significant imperfect attributes that need improvement to achieve similar low-temperature performance compared to the conventional multigrade mineral oil 15W40. Researchers have taken a variety of approaches to the challenge of CCO flow improvement with numerous additives and methodologies. For example, polymethylmethacrylate (PMMA), a polymer available in a range of molecular weights, has been used widely as a pour point depressant (PPD) and viscosity modifier (VM) [5–7]. In addition, sunflower oil (SF), styrenated phenol (SP), and oleic acid (OA) have also been used to reduce the PP of CCO [5,8]. Zinc-dialkyldithiophosphate (ZDDP) is used as a multi-purpose additive, which acts as a VM, anti-oxidant (AO), friction modifier (FM), anti-wear (AW) agent, and as a dispersant in the contemporary mineral-based lubricant industry [6,9,10]. PMMA is used in this work as a PPD and VM because of its

* Corresponding author.
E-mail address: james.bowen@open.ac.uk (J. Bowen).

https://doi.org/10.1016/j.triboint.2023.109060
Received 28 June 2023; Received in revised form 10 October 2023; Accepted 28 October 2023
Available online 31 October 2023

Table 1
Sample descriptions and compositions of chemicals used as PPD to reduce the PP of CCO.

S/N	Sample no	Composition				
		Base stock		PPD		
		CCO		PMMA	SF	SP
		(wt%)	(v/v%)	(wt%)	(v/v%)	(v/v%)
1	**L1**	99.75	x	0.25	x	x
2	**L2**	99.50	x	0.50	x	x
3	**L3**	99.25	x	0.75	x	x
4	**L4**	99.00	x	1.00	x	x
5	**L5**	x	95.00	x	5.00	x
6	**L6**	x	90.00	x	10.00	x
7	**L7**	x	85.00	x	15.00	x
8	**L8**	x	80.00	x	20.00	x
9	**L9**	x	95.00	x	x	5.00
10	**L10**	x	90.00	x	x	10.00
11	**L11**	x	85.00	x	x	15.00
12	**L12**	x	80.00	x	x	20.00

Key: CCO – coconut oil, PPD – pour point depressant, PMMA – polymethylmethacrylate, SF – sunflower oil, SP – styrenated phenol,

entangling behaviour [5–7]. SF is used as a PPD to create branches in CCO molecular structure because of its rich unsaturated (91.4%) molecular structure [1,5]. Similarly, SP is used as a PPD because of its hydroxyl functional groups, also to create branches to reduce the PP of CCO [5]. ZDDP, and KOH are additives blended with CCO to enhance its other properties. Nevertheless, there is no evidence of research using PMMA and SP together as a combined PPD to reduce the PP of CCO.

2. Experiment methodology

2.1. Materials

CCO was procured from local mills in Sri Lanka, and SF, SP, and OA were supplied by GlorChem Enterprise, Sri Lanka. Conventional mineral-based multigrade engine oil 15W40 was selected as the reference oil to govern the tests and purchased from the Ceylon Petroleum Cooperation (CEYPETCO), Sri Lanka. All other chemicals including antioxidants and viscosity modifiers were procured either from Sigma-Aldrich UK or Fisher Scientific UK.

2.2. Pour point depression of CCO

Three chemicals - PMMA ($M_w \sim 15{,}000$ g mol^{-1}), SF, and SP - were blended with CCO in different concentrations; 4 wt concentrations (0.25. 0.50, 0.75 and 1.0 wt%) of PMMA because of its powder form and 4 vol concentrations (5, 10, 15 and 20 v/v%) of SF and SP, because of their liquid state at ambient conditions; sample descriptions and composition of chemicals used are presented in Table 1. All twelve mixtures, each 10 ml volume, underwent blending using an ultrasonic mixer (Kerry - KS 200) for 1 h followed by 2 h of further agitation using a magnetic stirrer hotplate (Thermo Scientific – Cimarec^{+}) at 800 rpm and 150 °C in order to achieve homogeneous formulations.

PMMA and SP were added to CCO with reference to Ajithkumar et al.'s observations [5] and SF was added because of low PP (−12 °C) [1,5] and high (91.14%) unsaturated FA concentration [18:1, OA – 28.0%, 18:2, linoleic acid – 62.2%)].[1] Subsequently, all samples were analyzed via differential scanning calorimetry (DSC). The best formulation from each category was further tested using a Pour Point Tester (Stanhope – Seta) following ASTM D97–96a standard procedures.

DSC is the study of observing enthalpy changes thereby illustrating exothermic and endothermic processes, i.e., the heat-dissipating and heat-absorbing characteristics of a material. Two instruments were utilized for DSC testing: "Discovery–TA DSC 25″ and "Q2000 DSC". Two types of thermal analysis profiles were studied, specifically cooling and

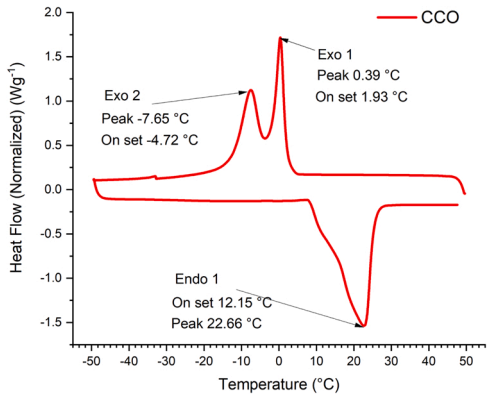

Fig. 1. DSC thermogram of CCO; Key: Exo – exothermic, Endo – endothermic.

heating experiments with the following procedures: 1) **exothermic tests:** Sample and reference were heated up to 50 °C and held isothermally for 10 min before cooling at a steady rate of 10 °C min^{-1}, until the sample and reference reached − 50°C; 2) **endothermic tests:** After the sample and reference reached − 50 °C (at the end of exothermic test), both were heated at a constant rate of 10 °C min^{-1}, until reaching 50 °C.

Improving viscosity, oxidative stability, and total base number (TBN) of CCO: PMMA has been shown to be a good viscosity modifier [6,11] and thus, 0.5 and 1.0 wt% concentrations of PMMA were added to the best CCO/PPD combination. The kinematic viscosity of the formulations were measured at 40 °C and 100 °C using a "Stanhope-Seta KN6″ capillary tube viscometer and an "Ambica T8006 B" Redwood viscometer. Enhancing the TBN or strengthening the alkalinity of a lubricant above the TAN is an effective remedy to maintain oil neutralization, which is the deciding factor for its life cycle [12]. Inhibiting oxidative stability will minimize acidic substance formation, hence minimizing erosion between sliding interfaces and preventing excessive wear [13]. In addition to its AO and AW properties and its use as a FM and VM, ZDDP is a good dispersant and works in synergy with other additives [14]. Therefore, ZDDP was added in 0.5, 1.0, 1.5, 2.0, 2.5 and 3.0 wt% concentrations as a multi-purpose additive after improving the PP of CCO.

Thermal analyses: Thermogravimetric analysis (TGA) and DSC tests were used to study the thermal and oxidative stability of the blends (Rheometric Scientific STA1500; TA Instruments–Q2000 DSC). TAN and TBN were tested via titration using a "Metrohm Titrino Plus 848″ analyzer following ASTM D664–18 and ASTM D 2896–21 respectively [15]. KOH was added in 0.25, 0.50, and 1.00 wt% concentrations to the optimal CCO/PPD formulations and tested for TAN and TBN following the same procedure. The final product, hereafter referred to as formulated coconut oil (FCO) was characterized via FT-IR analysis (Shimadzu IR-Affinity 1) for identifying the functional groups associated with the structure of CCO.

Rheological behaviour: The rheological behaviour of FCO was examined using a cone and plate (CP 4°/40 mm) rheometer (Bohlin/Gemini 2 – GEM200 – 903). The test protocol consisted of a series of shear rate sweeps, performed at 20 °C increments over the temperature range 60–120 °C.

Friction tests: Friction tests were implemented using a Linear Reciprocating Tribometer (LRT) test rig (DUCOM TR – 282) to analyse the lubricity of formulated coconut oil (FCO) along with engine oil (15W40) and compared. Piston ring and cylinder liner segments of an internal combustion engine (ICE) were used as test specimens to have a similar hardness to simulate real ICE operation. All the LRT tests were performed as per the ASTM G181–11 standards. The test protocol is with 2 variables: 5 different reciprocating velocities referenced to sliding frequencies (15, 20, 30, 40, and 50 Hz) with 5 different loads (120, 140, 160, 180, and 200 N), giving a total of 25 load/velocity combinations at 140 °C with 360 s duration for each test, totalling 2.5 h for the sequence.

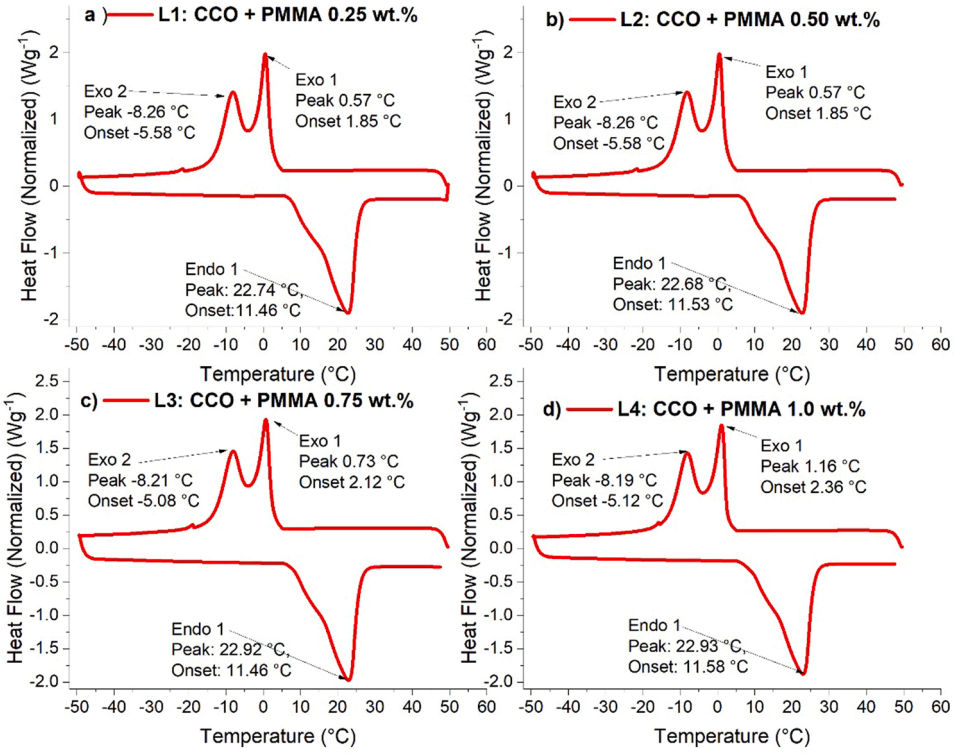

Fig. 2. DSC thermograms for the formulations having CCO with different concentrations of PMMA; a) L1: CCO + PMMA 0.25 wt%, b) L2: CCO + PMMA 0.50 wt%, c) L3: CCO + PMMA 0.75 wt%, d) L4: CCO + PMMA 1.00 wt%,.

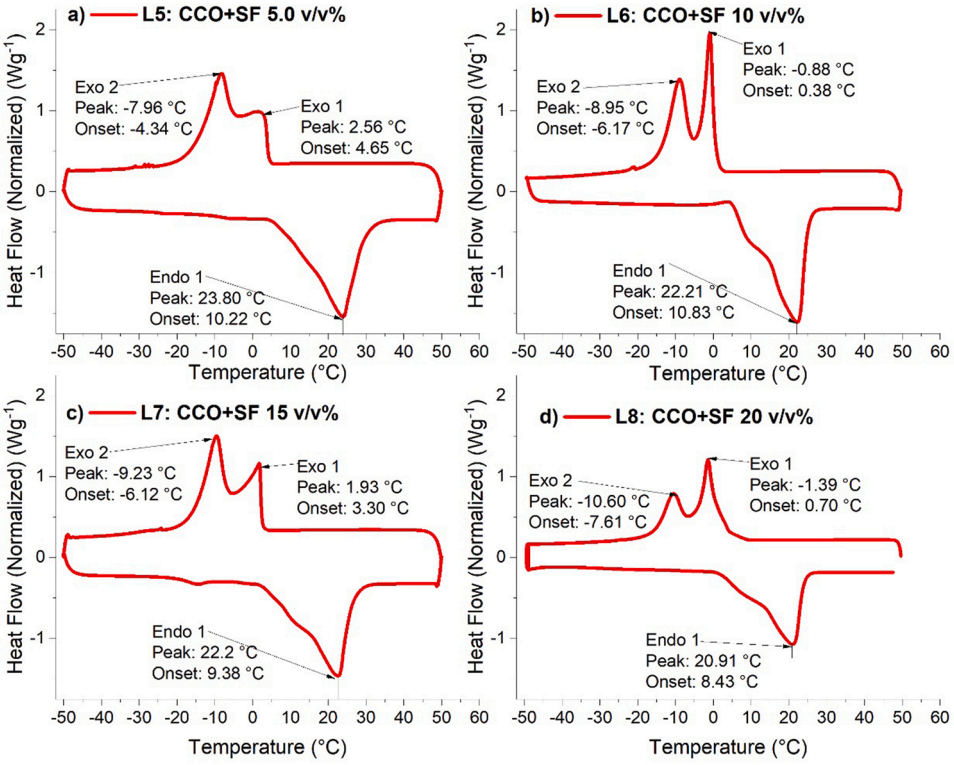

Fig. 3. DSC thermograms for the formulations having CCO with different concentrations of SF; a) L5: CCO+SF 5 v/v%, b) L6: CCO+SF 10 v/v%, c) L7: CCO+SF 15 v/v%, d) L8: CCO+SF 20 v/v%,.

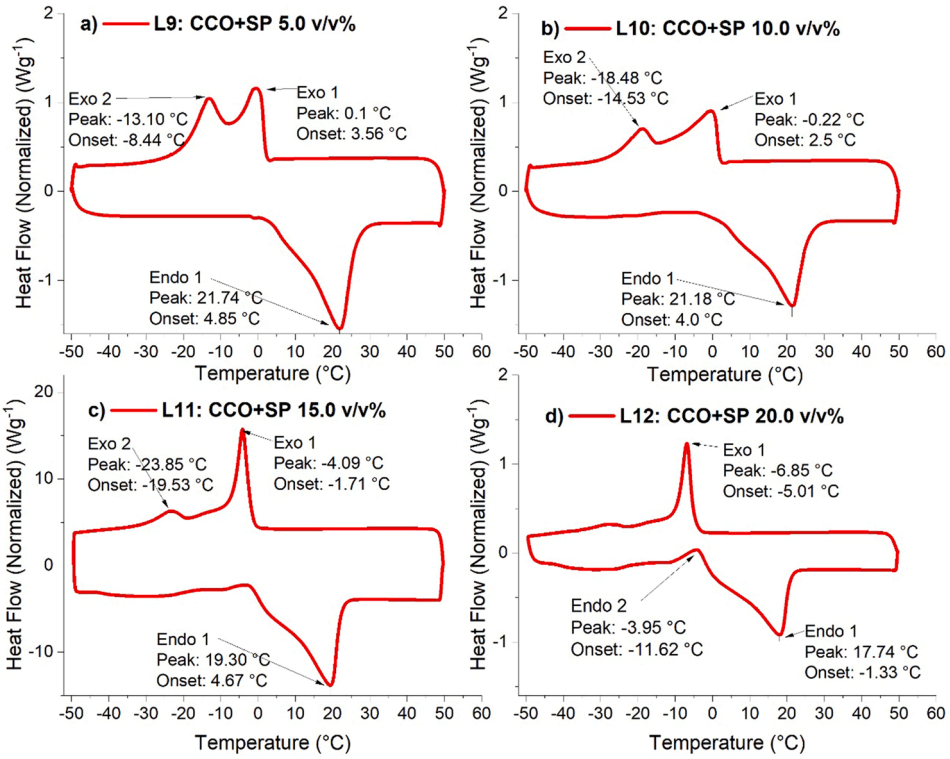

Fig. 4. DSC thermograms for lubricant samples containing CCO with different concentrations of SP; a) L9: CCO + SP 5 v/v%, b) L10: CCO + SP 10 v/v%, c) L11: CCO + SP 15 v/v%, d) L12: CCO + SP 20 v/v%.

3. Results and discussion

3.1. Improving physicochemical properties of CCO

Fig. 1 presents the DSC thermogram for the CCO. There are two exothermic peaks, labelled CCO_{Exo1} and CCO_{Exo2}, presenting maxima at 0.4 °C and − 7.7 °C, with 1.9 °C and − 4.7 °C respectively signifying two crystallization points. The different crystallization points could be attributed to different crystal phases (creating polymorphs) of complex triglyceride molecules of CCO [5]. There is one endothermic peak: CCO_{Endo1} at 22.7 °C with onset temperature 12.2 °C, which represents the melting of CCO.

From the DSC thermograms of formulations containing different concentrations of PMMA (Fig. 2), samples L1 and L2 have the lowest onset temperature endothermic peak at 22.7 °C and a peak maximum at 11.5 °C ($L2_{Endo1}$, Fig. 2b). However, there is little difference between the four thermograms in Fig. 2, which suggests that the concentration of PMMA used here does not significantly alter the thermal properties of the formulation. The endothermic peak transition temperature (EPTT), which represents the pour point (PP) of the fluid is almost the same for all four formulations and is similar to the EPTT for CCO (Fig. 1). The $L2_{Endo1}$ onset temperature, which indicates the onset of melting, was observed to shift marginally from 12.2 °C (CCO) to 11.5 °C. Similar results were observed from exothermic regions of DSC thermograms, which indicate the beginning of solidification with reference to the monitored $L2_{Exo1}$ and $L2_{Exo2}$ peak and onset temperatures.

DSC thermograms for sample blends combining different concentrations of SF with CCO (Fig. 3) show that sample L8 exhibits the lowest endothermic peak (20.9 °C) and onset temperature (8.4 °C), representing a 1.8 °C reduction of PP with ~ 3.7 °C shifted at the beginning of melting compared to CCOEndo1 (Fig. 1). From the $L8_{Exo1}$ and $L8_{Exo2}$ values it is evident that the beginning of the crystallization process has been shifted by ~1.2 °C and ~2.9 °C with peak maxima at − 1.4 °C and − 10.6 °C respectively compared to the CCO_{Exo1} and CCO_{Exo2} peak

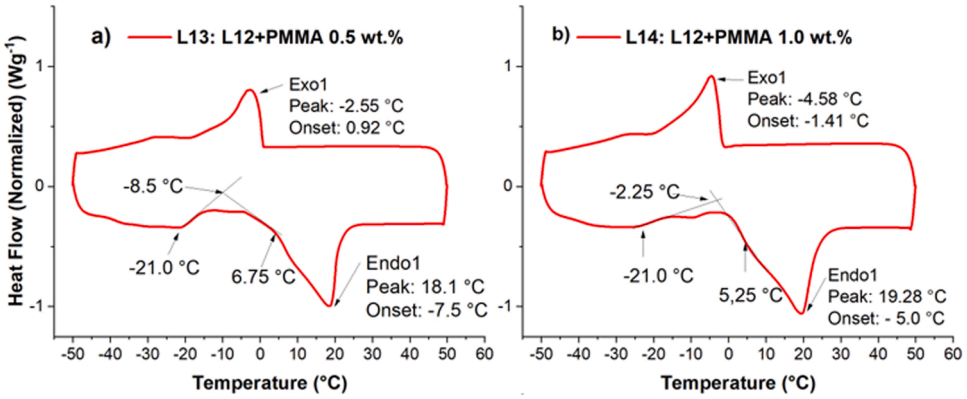

Fig. 5. DSC thermograms for sample blends having L12 with two concentrations of PMMA.

Table 2
Sample descriptions for formulations L13 and L14 which are having L12 with different concentrations of PMMA.

	Composition		
Sample code	Base oil	Additive	wt%
L13	L12	PMMA	0.5
L14	L12	PMMA	1.0

Table 3
Summary of PP for selected samples from each PPD group and Endo1 peak and onset values during the DSC endothermic process for the same.

Sample no	Pour point* (°C)	DSC - Endo 1	
	ASTM D97-96A	Peak (°C)	Onset (°C)
CCO	21	22.7	12.2
L2	21	22.7	11.5
L8	21	20.9	8.4
L12	15	17.7	-1.3
L13	6	18.1	-7.5
L14	9	19.3	-5.0

*Measured in 3 °C intervals

maxima (0.4 °C and −7.7 °C, Fig. 1).

Among all twelve DSC samples with three different PPDs, sample L12 shows a particularly impressive improvement in the cold flow behaviour of CCO, presenting a ~ 5.0 °C difference in peak position between CCO_{Endo1} and $L12_{Endo1}$ (Figs. 1 and 4d). In-addition, the $L12_{Endo1}$ onset temperature is reduced to − 1.3 °C, representing a ~ 13.5 °C shift in the beginning of melting compared to CCO. Moreover, $L11_{Exo2}$ (Fig. 4c) shows a broadened peak at − 23.9 °C. Sample L12 does not exhibit a second exothermic peak during cooling. Instead, there is an additional exothermic peak during the heating phase with peak and onset temperatures of − 4.0 °C and − 11.6 °C respectively (Fig. 4d). This signifies the recrystallization of low melting polymorphs to high melting polymorphs [hexagonal subcell (α) – orthogonal subcell (β') – triclinic subcell (β)] before commencing the melting process [5,6]. From the results obtained during cooling of CCO and L12, it is evident that the onset of $L12_{Exo1}$ has been lowered by ~ 6.9 °C compared to the onset of CCO_{Exo1}, confirming the improvement of cold flow.

Fig. 5 illustrates the DSC thermograms for sample blends L13 and L14 consisting of L12 with added PMMA at concentrations 0.5 wt% and 1.0 wt%. Sample codes and descriptions of these two formulations are presented in Table 2. Neither sample exhibits an Exo2 peak during cooling, in contrast to CCO (Fig. 1), confirming crystallization into the low melting temperature *"α"* crystalline form [5,6]. Both blends present a broadened exothermic peak, between − 21.0 to 6.75 °C (L13) and between − 21.0 to 5.25 °C (L14), confirming a change of crystallization mechanisms and melting patterns for these formulations compared to CCO.

Pour point (PP) is the parameter used to define the cold flow behaviour of liquid lubricants tested in accordance with ASTM D97–96A guidelines, whereas DSC analysis provides in-depth understanding on the behaviour of a fluid under different thermal conditions. The PP of the samples with the best performance from each PPD group (L2, L8 and L12) and of both L12/PMMA samples (L13 & L14) were tested following ASTM D97–96A. The test results in Table 3 show that L13 has the optimum cold flow behaviour with PP at 6.0 °C, a reduction of 15 °C compared to CCO, even though the endothermic peak of L13 remains at 18.1 °C. However, this improvement could be ascribed to the commencement of melting at a lower temperature (−7.5 °C – Endo1 onset) and continuing up to 18.1 °C ($L13_{Endo1}$ peak), as the formulation passes through many transition phases, evident from the broadened exothermic peak during heating, before reaching the liquid state. Thus, it is assumed that liquid flow will start within this range, presenting a lower temperature PP than the value of the endothermic peak shown in the DSC thermogram.

Fig. 6a illustrates the overlay of DSC thermograms for the samples CCO and L13, which clearly indicate the change in exothermic and endothermic traces illustrating the enhancement in the low-temperature flow behaviour of CCO.

FT-IR spectra for CCO, L13, and SP (Fig. 6b) confirm the anticipated variety of oxygen functional groups (carbonyl, carboxyl, hydroxyl) within their molecular structures, L13 presenting more IR bands than CCO. A broad peak (3600 cm^{-1} – 3300 cm^{-1}) could be ascribed to OH stretching (phenol or alcohol) and the peak at 1600 cm^{-1} could be C═C stretching vibration (alkene – aliphatic/aromatic). Additional bands in the range of 800–500 cm^{-1} could be assigned to C-H or C═C bending vibrations. The results could be attributed to the addition or amalgamation of functional groups (SP and PMMA) to the CCO structure, noting that the major constituents of CCO are the saturated fatty acids; dodecanoic (lauric) acid (47.7%) and tetra-decanoic (myristic) acid (19.9%) (Essential Supplementary Information [ESI] Table S1). Thus, it is proposed that formulation L13 improves the poor cold flow characteristics of CCO by entangling or creating branches with the molecular structure, inhibiting macro-crystallization thus causing micro-crystallization and impeding self-molecular stacking [5,6,16], a mechanism which aligns with Minami's assumption [6]. The specifications of the CCO constituents are listed in ESI Table S1.

Improving VI of formulated CCO: After improving the cold flow behaviour of FCO attention turned to its flow properties. The kinematic viscosities of sample formulations were tested at 40 °C and 100 °C following ASTM D445–19a standard methods. Sample L12, and both L12/PMMA samples (L13 & L14) were selected for this investigation. Measured viscosity values are used to evaluate the VI of formulations

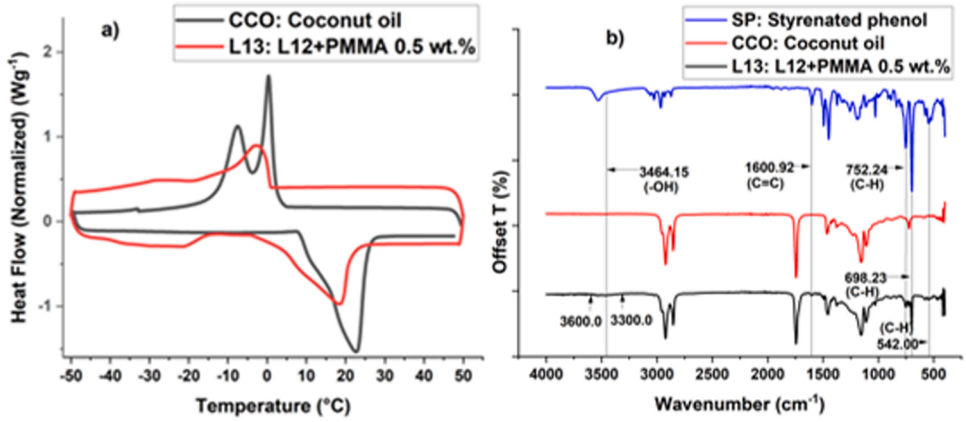

Fig. 6. Overlay of DSC, and FT-IR for CCO and SP2/P05; a) DSC thermograms, b) FT-IR spectrometry curves.

Table 4
Summary of TBN test results for the formulations containing L12 with different concentrations of PMMA and KOH.

Sample no	Composition	TBN (mg KOH g^{-1})
L12	CCO + SP 20 v/v%	0.23
L13	L12 + PMMA 0.5 wt%	0.16
L14	L12 + PMMA 1.0 wt%	0.13
L15	L13 + KOH 0.25 wt%	1.74
L16	L13 + KOH 0.50 wt%	4.14
L17	L14 + KOH 0.25 wt%	0.86
L18	L14 + KOH 0.50 wt%	1.66

Table 5
Comparison of physicochemical properties of FCO vs CCO and 15W40.

Sample	TAN (mg KOH g^{-1})	TBN (mg KOH g^{-1})	KV @ 40 °C ($mm^2 s^{-1}$)	KV @ 100 °C ($mm^2 s^{-1}$)	VI ()	PP* (°C)
CCO	1.94–12.8	****	24.8	5.5	169	21.0
FCO	0.29	4.14	46.2	9.8	206	6.0
15W40	****	9.8	109	14.1	130	-33.0

Key: TAN – total acid number, TBN – total base number, KV – kinematic viscosity, VI – viscosity index, PP – pour point; * measured in 3 °C intervals

adhering to ASTM D2270 directives. The results are presented in (ESI) Table S2, which confirms the ability of polymers to modify the lubricant viscosity making it less sensitive to variations in operating temperatures. Sample L14 (VI: 260) is more effective in increasing VI than L13, however, L13 (VI: 206) is more successful in improving cold flow behaviour than L14. Nevertheless, these results confirm the ability of polymers having large, entangled chains to improve the VI of a mixture, making the formulation less sensitive to increasing temperatures [6,7]. The mechanism could involve a globule–to–random coil transition, which depends on the attractive or repulsive interactions between formulation molecules and polymer chain segments, because of its thermal coil expansion behaviour [6,11,17].

Improving TBN of formulated CCO: The TBN of the sample blends were tested after adding ZDDP as elucidated in the methodology. All six ZDDP concentrations caused a change to the TBN. Sample L12 (without ZDDP) exhibited a TBN of 0.23 mg KOH g^{-1}, which decreased slightly to 0.15 mg KOH g^{-1} upon the addition of ZDDP. In contrast, adding ZDDP to L12 increased the TAN from 0.29 mg KOH g^{-1} to 5.1 mg KOH g^{-1} (ESI Table S3). This outcome could be assigned to an interaction between the dithiol group of ZDDP with the carboxyl, phenol, and alkyl functional groups of CCO and SP. In view of these results, three different concentrations (0.25, 0.50, and 1.0 wt%) of KOH were added to formulations L13 and L14, because of the expected cold flow improvement. Sample codes, descriptions and test results are presented in Table 4. TBN was tested according to ASTM D2896–21.

The results indicate that the addition of PMMA to L12 has reduced the TBN (L13, L14, Table 4), an effect which might be attributed to the combination of carbonyl and hydroxyl groups of PMMA and SP respectively by chemical reaction, generating more carboxyl groups in the formulation. Sample L16 exhibited improved TBN of 4.14 mg KOH g^{-1} (Table 4), albeit adding 1.0 wt% of KOH resulted in saponification. Hence, formulation L16 was given the assignation formulated coconut oil (FCO), which is constituted with 99.5% of L13 + KOH 0.50 wt%. The formulation L13 is constituted with 99.5% of L12 + PMMA 0.50 wt%. Thus, the chemical composition of FCO (L16) is CCO 76.8 wt% + SP 22.2 wt% + PMMA 0.5 wt% + KOH 0.5 wt% assuming the densities of CCO and SP are 0.925 and 1.07 g cm^{-3} respectively. This formulation was used for further investigations. Comparison of achieved physicochemical properties of FCO with CCO and 15W40 are summarized in Table 5.

Thermal and oxidative stability of FCO was analysed with two gaseous environments to differentiate between oxidative and anoxic

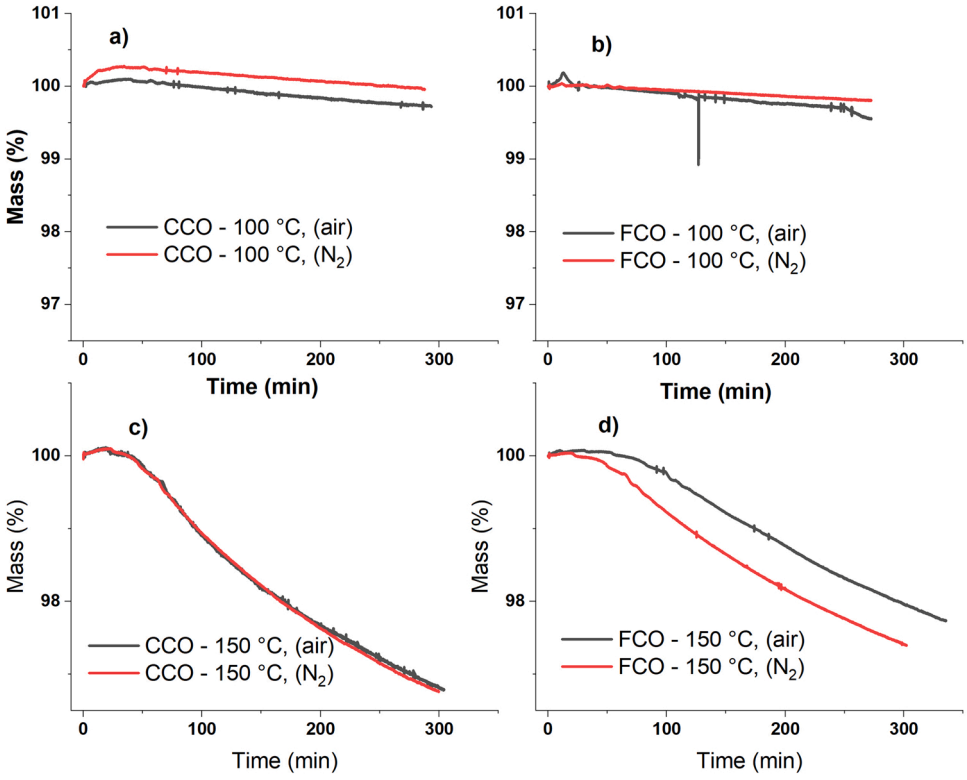

Fig. 7. TGA thermograms for weight loss analysis on CCO and FCO at 100 °C and 150 °C under dissimilar environments; a) CCO at 100 °C, b) FCO at 100 °C, c) CCO at 150 °C, d) FCO at 150 °C.

Table 6
Summary of oxidative and anoxic thermal stability of CCO and FCO at 100 °C and 150 °C.

Sample	Mass loss after 5 h (%)					
	Temperature (100 °C)			Temperature (150 °C)		
	Air	N_2	Oxidation%	Air	N_2	Oxidation%
CCO	0.28	0.05	0.23	3.22	3.24	-0.02
FCO	0.45	0.20	0.25	2.26	2.60	-0.34

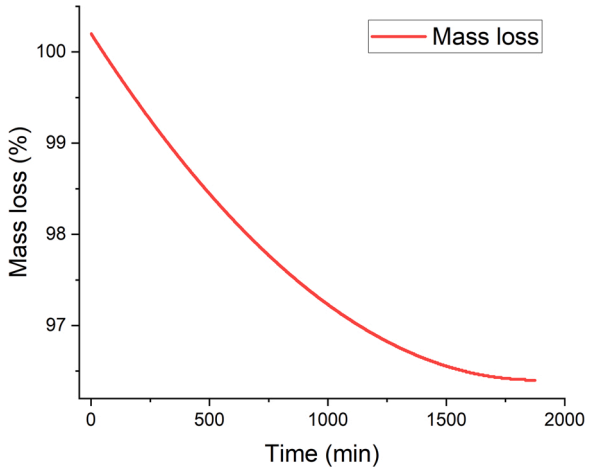

Fig. 8. TGA thermogram for FCO under naturally aspirated environment for extended hours at 120 °C.

thermal degradation of sample formulations. Peak Scientific Zero Air (79.1:20.9 N_2:O_2, volume basis) and inert gas (N_2) were the gas environments chosen for comparison using TGA. Any mass loss measured in the presence of O_2 could be attributed to a combination of oxidative and anoxic thermal degradation. Conversely, mass loss under N_2 could only be assigned to anoxic thermal degradation [18–20]. Fig. 7 presents the TGA thermograms for CCO and FCO held at 100 °C and 150 °C under O_2-containing and O_2-free atmospheres. Fig. 7d shows that the FCO displays similar mass loss under both gas flows and confirms the thermal stability of FCO in air. Referring to Table 6, FCO displays a slightly better thermal and oxidative stability than CCO, which could be caused by the presence of the chemicals added to improve physicochemical properties. Suggested mechanisms to improve poor cold flow are the creation of branches to the CCO molecular structures or the entanglement of CCO molecules. A possible explanation for the effect on thermal stability is that adding branches creates supplementary unsaturated C=C bonds.

Long hold TGA was performed on FCO at 120 °C for 31 h. The results revealed a 3.6% mass loss over ~30 h under isothermal condition, before the solution become stable in terms of mass loss (Fig. 8). FCO seems stable at 100 °C in terms of thermal and oxidative degradation (Fig. 7). The operating temperature of an ICE will range from 80°C to 105°C, and if engine temperature increases above 105 °C, will be shut down as a safety feature, thus degradation of FCO above 100 °C was not considered.

Rheological analysis of the shear stability of FCO: Fig. 9 shows the shear stability of both FCO and 15W40 at temperatures of 60, 80, 100, and 120 °C. Both samples display similar pseudoplastic characteristics in the shear rate range ~ 5×10^2 to 7×10^3 s^{-1} for all test temperatures. In addition, two different flow behaviours are visible at two different ranges of shear rate: a) a viscosity reduction over the shear rate range ~ 0 to 5×10^2 s^{-1}, and b) a small viscosity reduction across the shear rate range ~ 5×10^2 to 7×10^3 s^{-1}. However, there is no clearly visible effect of the changes in temperature on the lubricant properties. Plotting the results on log-log axes instead of linear-linear axes may reveal new insights into their flow characteristics. The power-law model was fit to the data in order to analyse the flow behaviour of selected sample lubricants. Typical peak shear rates for piston rings within a working engine can be as high as 2×10^7 s^{-1} (far in excess of the shear rates achievable here) although temperatures are generally between 80 °C and 105 °C [21].

Power-law (Ostwald-de Waele) model: This model is appropriate for fitting the rheometric behaviour of non-Newtonian lubricants, which exhibit pseudoplastic behaviour or the measured data is entirely within the shear thinning regime. Proportionality between shear stress (σ) and change of shear stress [shear rate or velocity gradient] ($\dot{\gamma}$) is defined as the shear viscosity or dynamic viscosity (η). With reference to power-law model (Eq. 1), these parameters are combined to predict the characteristics of the fluid using flow curves [22,23].

Power-law equations [22,23]:

$$\sigma = K\dot{\gamma}^{n} \tag{1}$$

$$\eta = \frac{\sigma}{\dot{\gamma}} = K\dot{\gamma}^{(n-1)} \tag{2}$$

Where: K – Flow consistency index (or dynamic viscosity when shear rate is 1 ($\log \dot{\gamma} = 0$) with units (Pa s^n).

n – The flow behaviour index (dimensionless).

Fig. 10 presents the flow behaviour of FCO under ramping shear rates in double log scale for different temperatures (60, 80, 100, and 120 °C). Flow curves indicate similar characteristics for all temperatures. The linear section of curves indicates the power-law region, where the points A (3.57, −2.13) and B (2.10, −1.45) are marked.

From these points the gradient for the power-law region is − 0.462, and since the gradient of the power-law region is $= n - 1$ (Eq. 2).

Therefore $n = 0.538$, confirming the pseudoplasticity ($n < 1$) of the liquid in the log shear rate range 2.0–3.7 (10^2 s^{-1} to 7×10^3 s^{-1}). The

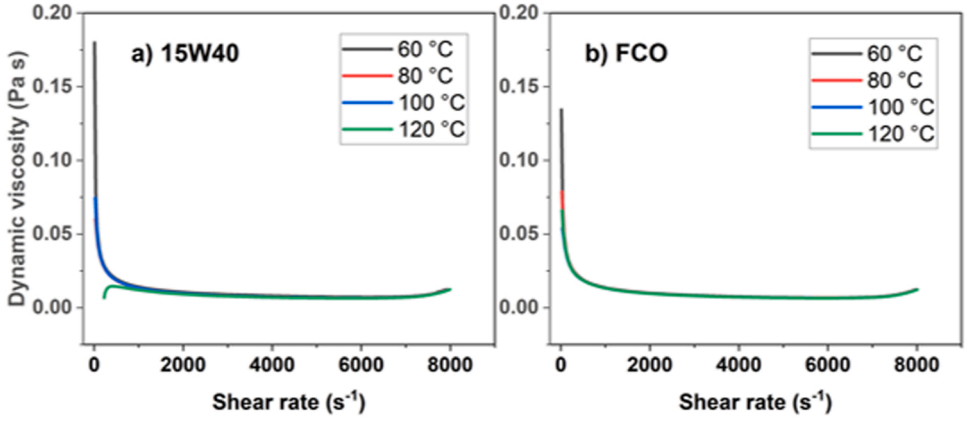

Fig. 9. Rheometric curves in linear-linear axes for a) reference oil (15W40), and b) FCO.

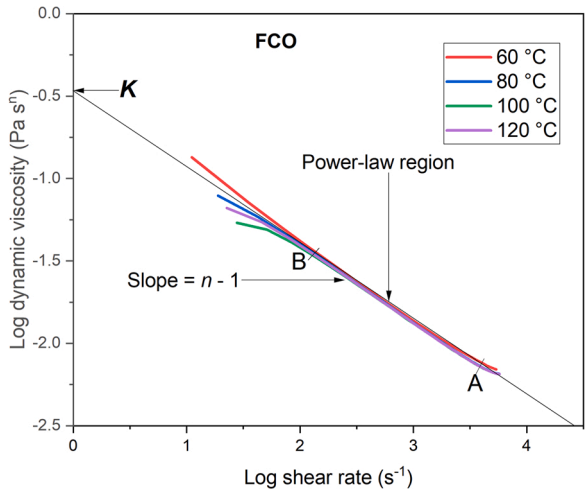

Fig. 10. Rheometric curves of FCO in log – log axes under ramping shear rates in different temperatures (60, 80, 100, and 120 °C, AB – the range of shear thinning).

Table 7
Calculated flow behavior index (n) for FCO and 15W40.

Parameter	Sample	
	FCO	**15W40**
Gradient (*n*-1)	-0.463	-0.473
n	0.537	0.527

Note: "*n*" denotes the flow behaviour index

value of "***n***" for 15W40 also confirms the shear thinning performance due to the presence of a similar power-law region. Both ***"n"*** values for FCO and 15W40 are listed in Table 7. In addition, from Eq. 2 it is observed that the flow consistency index ***K*** could be defined as follows:

$$\log\eta = \log K + (n-1)\log\dot{\gamma} \tag{3}$$

$$\therefore \log\ \eta = \log\ k, \text{ when } \dot{\gamma} = 1, (\log\ \dot{\gamma} = 0) \tag{4}$$

Therefore, the intercept of the power-law gradient line at log $\dot{\gamma} = 0$ (value of y axis where x = 0) will give the value of ***K***.

Fig. 11 presents the flow behaviour of 15W40 and FCO with similar shear-thinning characteristics indicated for all temperatures.

FCO exhibits greater shear stability than 15W40, an effect which could be attributed to the addition of PMMA as a viscosity modifier. PMMA consists of large molecular chains with the capability to entangle with the solvent molecules. This results in an improved viscosity dependence on temperature for FCO, which exhibits an enhanced VI compared to 15W40 and CCO (Table 5) [6,24]. If shear-thickening does not occur, most non-Newtonian fluids will reach a viscosity plateau at high shear rates according to Carreau-Yasuda and Cross model predictions [23]. On the other hand, shear-thickening is critical at high shear rates to maintain lubricant viscosity in real ICE operation.

Observations of friction tests: Fig. 12 shows the COF vs time analysis for FCO and reference oil (15W40) under two different test conditions, a) 120 N load with 20 Hz of sliding frequency and b) 180 N load with 50 Hz of sliding frequency, both at 140 °C elevated temperature. The results indicate that the FCO is capable of reducing the COF by 7% (mean) for all 25 test conditions with maximum COF reduction of 53% under the test "b)" without adding any additives.

4. Conclusions

The separate addition of PMMA or styrenated phenol (SP) to coconut oil (CCO) did not improve the cold flow behaviour of CCO. However, adding both PMMA and SP together improved the cold flow characteristics of CCO, reducing its pour point (PP) by 15 °C, from 21 °C to 6 °C. It is presumed that both entangling and adding branches to the CCO formulation inhibits macro crystallization, promotes micro crystallization, and impedes molecular self-stacking. This hypothesis is suggested by the results of differential scanning calorimetry tests which displayed a change in the crystallization and melting patterns of formulated coconut oil, i.e., CCO which contained both PMMA and SP. The addition of PMMA also improved the viscosity index of the CCO from 169 to 206 while the addition of KOH 0.5 wt% improved the total base number from 0 to 4.14 mg KOH g^{-1}. Thermogravimetric testing revealed that the formulated coconut oil exhibits better oxidative and thermal stability than CCO. Rheometric tests confirmed the acceptable shear stability of formulated coconut oil for engine lubrication applications, exhibiting similar shear stability to the conventional multigrade engine oil 15W40. Tribometry confirmed the improved lubricity of formulated coconut oil compared to the reference oil 15W40, with a 7% mean COF reduction for all 25 test conditions.

Statement of orignality

I, the Corresponding Author, declare that this manuscript is original, has not been published before and is not currently being considered for publication elsewhere. I can confirm that the manuscript has been read and approved by all named authors and that there are no other persons who satisfied the criteria for authorship but are not listed. I further confirm that the order of authors listed in the manuscript has been approved by all of us. I understand that the Corresponding Author is the sole contact for the Editorial process and is responsible for communicating with the other authors about progress, submissions of revisions

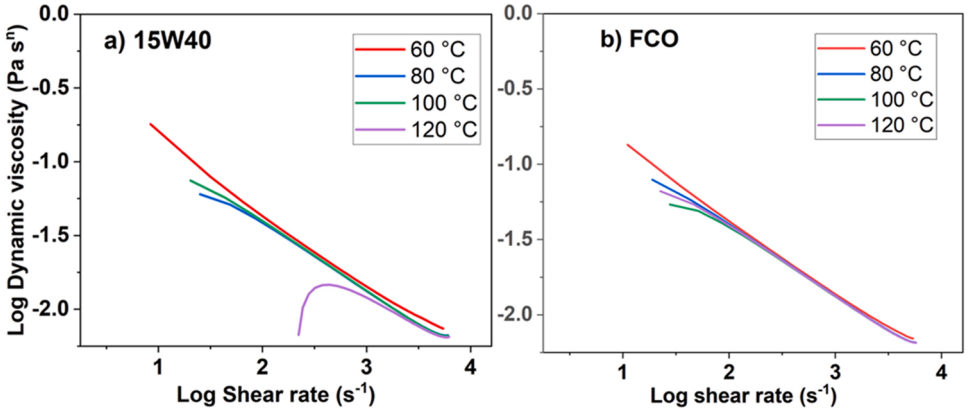

Fig. 11. Rheometric curves in log-log axes for a) reference oil (15W40), and b) FCO.

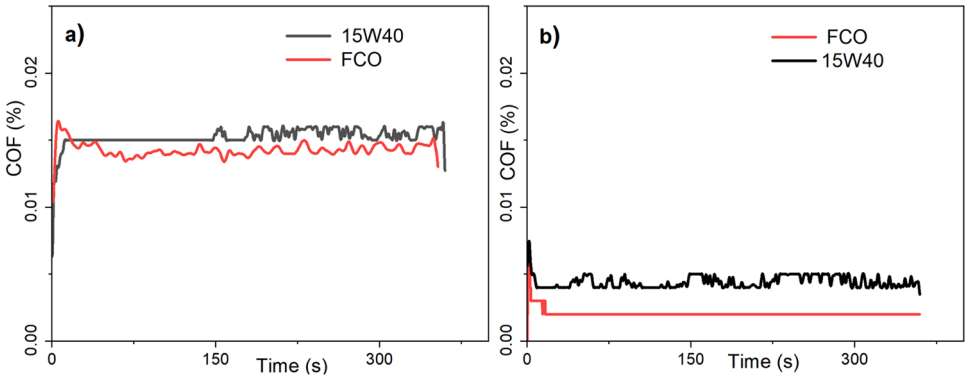

Fig. 12. Tribometry graphs for LRT tests; COF vs time analysis between FCO and 15W40 under two different test conditions, a) 120 N load with 20 Hz sliding frequency, b) 180 N load with 50 Hz sliding frequency, both at 140 °C.

and final approval of proofs.

Declaration of Competing Interest

The authors declare that they have no known competing financial interests or personal relationships that could have appeared to influence the work reported in this paper.

Data Availability

Data will be made available on request.

Acknowledgement

The authors acknowledge the technical support and analytical facilities at London South Bank University and the Open University, UK.

Appendix A. Supporting information

Supplementary data associated with this article can be found in the online version at doi:10.1016/j.triboint.2023.109060.

References

[1] Syahir AZ, et al. A review on bio-based lubricants and their application. J Clean Prod 2017;Vol. 168:997–1016.
[2] Zainal NA, Zulkifli NWM, Gulzar M, Masjuki HH. A review on the chemistry, production, and technical potential of bio-based lubricants. Renew Sustain Energy Rev 2018;Vol. 82(1):80–102.
[3] https://www.statista.com/statistics/613147/coconut-oil-production-volume-worldwide/ [Accessed: 21/02/2023].
[4] Gulzar, M., 2018. Tribological study of nanoparticle enriched bio-based lubricants for piston ring-cylinder interaction. Springer Theses. https://link.springer.com/book/10.1007/978–981-10–8294-8 [Accessed: 17/11/2020].
[5] Ajithkumar G, Jayadas MH, Bhasi M. Analysis of the pour point of coconut oil as a lubricant base stock using differential scanning calorimetry. Lubr Sci 2009;Vol. 21(1):13–26.
[6] Minami I. Molecular science of lubricant additives. Appl Sci 2017;Vol. 7(5):1–33. 445, pp.
[7] Whittle TJ, Leggett GJ. Influence of molecular weight on friction force microscopy of polystyrene and poly (methyl methacrylate) films: Correlation between coefficient of friction and chain entanglement. Langmuir 2009;Vol. 25:2217–24.
[8] Abdulrahiman, K.T.A., Sajeeb, A.M., 2019. Characteristical study of coconut oil-based nano-lubricant. International Conference on System Energy and Environment (ICSEE) 2019, GCE Kannur, Kerala, July 2019, Available at SSRN: https://ssrn.com/abstract=3438121 or https://doi.org/10.2139/ssrn.3438121.
[9] Spikes H. The history and mechanisms of ZDDP. Tribol Lett 2004;Vol, 17(3):469–89.
[10] Zhang J, Spikes H. On the mechanism of ZDDP antiwear film formation. Tribol Lett 2016;Vol. 63:9–24. Springer.
[11] Zhao Y, Li W, Wang X, Wang J. Tribological properties of trimellitates containing polymethacrylates viscosity modifiers. Proc IMechE Part J: Eng Tribology 2018;Vol. 232(7):882–9.
[12] Dorr N, Agocs A, Besser C, Ristic A, Frauscher M. Engine oils in the field: a comprehensive chemical assessment of engine oil degradation in a passenger car. Tribology Lett 2019;Vol. 67(68).
[13] Dong J, Van De Voort FR, Yaylayan V, Ismail AA, Pinchuk D, Taghizadeh A. Determination of total base number (TBN) in lubricating oils by mid-FTIR spectroscopy. J Soc Tribol Lubr Eng 2001;Vol. 57.
[14] Abere, J.O., 2017. Improved performance of bio-lubricants by nanoparticles additives. White rose e-theses, Sheffield, University of Sheffield. Available at: ⟨https://etheses.whiterose.ac.uk/18408/2/Julius%20O%20ABERE_PhD_2017.pdf⟩.
[15] Baig A, Paszti M, Flora TTNg. A simple and green analytical method for acid number analysis of biodiesel and biodiesel blends on potentiometric technique. Fuel 2013;Vol. 104:426–32.
[16] Voong M., 2005. Optimization of crankcase lubricant additive – material combination for reduced friction and wear in internal combustion engines, Edinburgh, Heriot-Watt University. Available at: ⟨https://www.ros.hw.ac.uk/handle/10399/162⟩.
[17] Covitch MJ, Trickett KJ. How polymers behave as viscosity index improvers in lubricating oils. Advances in Chemical Engineering and Sciences, Vol. 5. Scientific Research Publishing; 2015. p. 134–51.
[18] Boateng L, Ansong R, Owusu WB, Steiner-Asiedu M. Coconut oil and palm oil's role in nutrition, health and national development: a review. Ghana Med J 2016;Vol. 50(3):189–96. Available at: https://www.ncbi.nlm.nih.gov/pmc/articles/PMC5044790/pdf/GMJ5003-0189.pdf.
[19] Hsu, S.M., Cummings, A.L., 1983. Thermogravimetric analysis of lubricants. SAE: Lubricant and Additive Effects on Engine Wear – SP-558,
[20] Mosarof MH, Kalam MA, Masjuki HH, Arslan A, Monirul IM, Ruhul AM, et al. Analysis of thermal stability and lubrication characteristics of Millettia pinnata oil. RSC Adv 2016;Vol. 6:81414–25.
[21] Tailor RI, De Kraker BR. Shear rates in engines and implications for lubricant design. Proc IMechE, Part J: J Eng Tribology 2017;Vol. 231(9):1106–16.
[22] Sergio LDK, Soares EJ, Thompson RL, Siqueira RN. Friction coefficient of Bingham and power-law fluids in abrupt contractions and expansions. J Fluid Eng 2017;Vol. 139(2):21203–11.
[23] Azeez S, Bertola V. Lubrication of journal bearings by shear thinning lubricants using different constitutive models. Proc IMechE Part J: J Eng Tribol 2021;Vol. 235(6):1203–10.
[24] Stachowiak, G.W. , Batchelor, A.W. , 2005. Chapter 2: Physical properties of lubricants. Engineering Tribology, 3rd Ed., pp 41–50.